# Beyond the Helix Pitch: Direct Visualization of Native DNA in Aqueous Solution

Shinichiro Ido,[†] Kenjiro Kimura,[†] Noriaki Oyabu,[†] Kei Kobayashi,[‡] Masaru Tsukada,[§] Kazumi Matsushige,[†] and Hirofumi Yamada[†,*]

[†]Department of Electronic Science and Engineering and [‡]Office of Society-Academia Collaboration for Innovation, Kyoto University, Kyoto University Katsura, Nishikyo, Kyoto 615-8510, Japan and [§]WPI-Advanced Institute for Materials Research (WPI-AIMR), Tohoku University, Katahira 2-1-1, Aoba, Sendai, Miyagi 980-8577, Japan

ABSTRACT The DNA double helix was first elucidated by J.D. Watson and F.H.C. Crick over a half century ago. However, no one could actually "see" the well-known structure ever. Among all real-space observation methods, only atomic force microscopy (AFM) enables us to visualize the biologically active structure of natural DNA in water. However, conventional AFM measurements often caused the structural deformation of DNA because of the strong interaction forces acting on DNA. Moreover, large contact area between the AFM probe and DNA hindered us from imaging sub-molecular-scale features smaller than helical periodicity of DNA. Here, we show the direct observation of native plasmid DNA in water using an ultra-low-noise AFM with the highly sensitive force detection method (frequency modulation AFM: FM-AFM). Our micrographs of DNA vividly exhibited not only overall structure of the B-form double helix in water but also local structures which deviate from the crystallographic structures of DNA without any damage. Moreover, the interaction force area in the FM-AFM was small enough to clearly discern individual functional groups within DNA. The technique was also applied to explore the synthesized DNA nanostructures toward the current nanobiotechnology. This work will be essential for considering the structure—function relationship of biomolecular systems *in vivo* and for *in situ* analysis of DNA-based nanodevices.
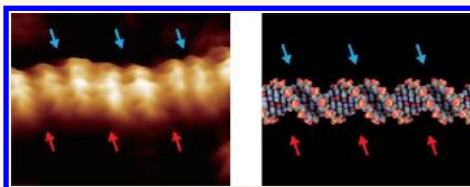
KEYWORDS: double-stranded DNA · frequency modulation atomic force microscopy · nanobioimaging · DNA nanotechnology · molecular self-assembly

Since the discovery of the double helix structure of DNA by Watson and Crick,[1] extensive efforts have been made to explore biological functions based on the DNA structure. Atomic force microscopy (AFM)[2] is one of the few real-space observation tools capable of visualizing biomolecular structures in solution. However, imaging the submolecular structure of double-stranded DNA by AFM has not been successful because of the poor ability to control interaction forces acting on DNA; only a few researchers have reported imaging of double-stranded DNA in solution, with limited spatial resolution in which grooves of double-stranded DNA were barely resolved.[3−5] Recently, AFM with frequency modulation detection method (FM-AFM)[6,7] has been used to observe more detailed DNA structures in solution.[8,9] However, there has been no information other than the helical symmetry of B-form DNA, which has already been determined by crystallographic studies.[1,10] Here, we directly visualize closed-circular plasmid DNA in an aqueous solution by using FM-AFM. The major and minor grooves were clearly resolved, and the highly improved force sensitivity allowed us to distinguish individual phosphate groups in the DNA backbones without sample deformation. In addition, we demonstrate sub-molecular-scale imaging of self-assembled DNA crystals[11] in an aqueous solution, which directly relate to DNA nanotechnology.[12,13]

Under physiological conditions, most double-stranded DNA (dsDNA) molecules adopt the B-form conformation.[14] B-form DNA (B-DNA) molecules have right-handed helical structures and distinctive major and minor grooves, which are ideally described by the well-known Watson—Crick model of DNA. The groove structures on the B-DNA surface are closely related to gene functions, such as formation of the nucleosome core[15] and control of gene expression by DNA-binding proteins.[16] We used FM-AFM, where the tip—sample interaction forces are measured as the
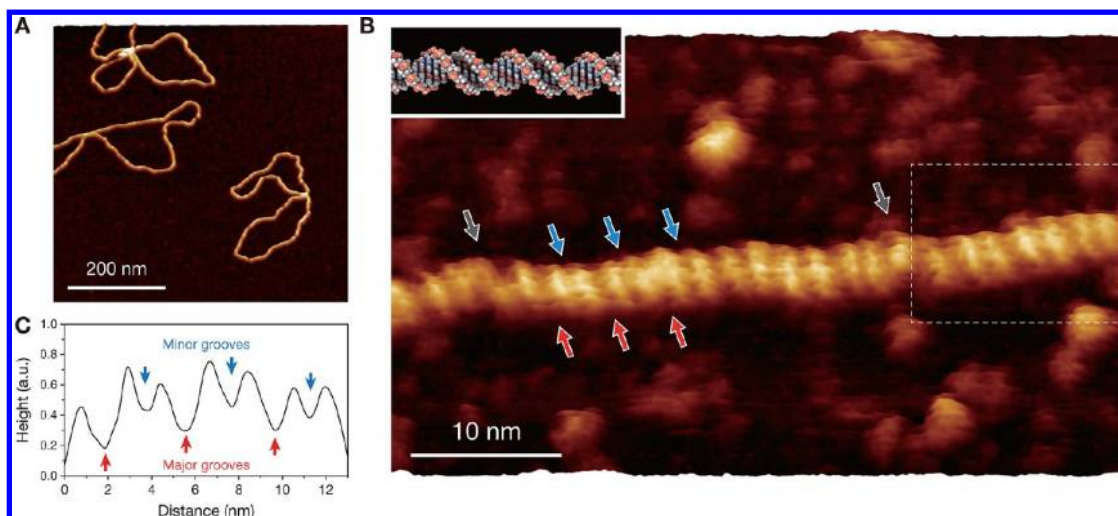
Figure 1. FM-AFM images of plasmid DNA. (A) Typical FM-AFM topographic image of the supercoiled structure of the closed-circular plasmid DNA (2686 base pairs) in aqueous solution (50 mM NiCl$_2$) (Supporting Information Figure S5). (B) High-resolution FM-AFM topographic image of the plasmid DNA in aqueous solution (50 mM NiCl$_2$). The red and blue arrows indicate the positions of major and minor grooves of B-DNA, respectively. Local melting regions of the plasmid DNA are indicated by gray arrows. Inset: molecular structure of the B-DNA. (C) Averaged cross-sectional profile along the helix axis of DNA measured in the area indicated by the white rectangle in (B) (Supporting Information Figures S6 and S7). The red and blue arrows indicate the positions of the major and minor grooves, respectively.
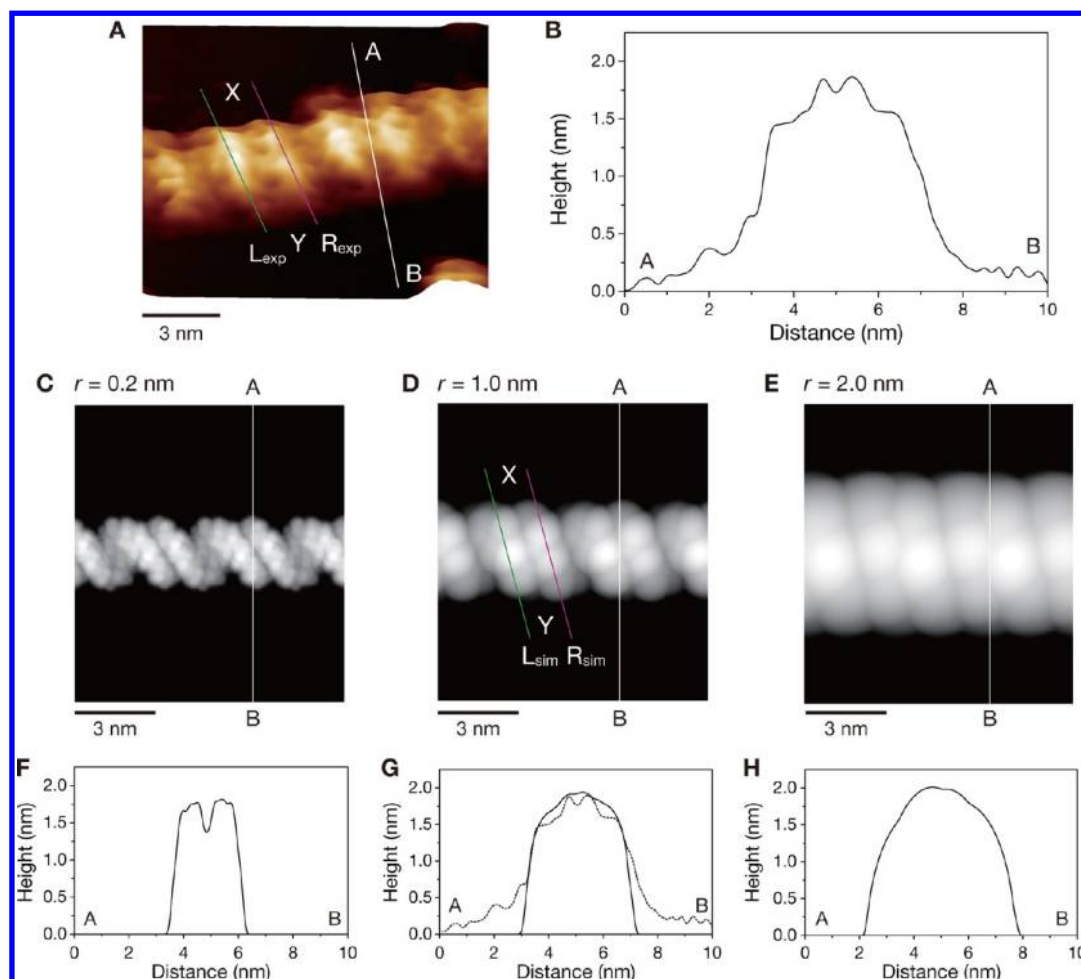

Figure 2. Comparison of the FM-AFM and simulated AFM images. (A) Magnified image of the area indicated by the white rectangle in Figure 1B. (B) Cross-sectional profile along the A–B line in (A), which is perpendicular to the helix axis. (C–E) Simulated AFM images of B-DNA assuming tips with a radius of 0.2, 1.0, and 2.0 nm. (F–H) Cross-sectional profiles along the A–B lines in (C–E), respectively, which are perpendicular to the helix axes. The profile in (B) is superimposed on (G) (dashed line).

resonance frequency shift of the self-oscillated canti-lever. The resonance frequency shift is sensitive to the forces acting on the probe tip at the closest approach distance to the sample surface during an oscillation cycle. The force sensitivity is enhanced compared with that of other conventional AFM methods, in particular, when the oscillation amplitude is reduced to the same order as the decay length of the interaction forces between the tip and sample.[7] Recently, we reported the use of FM-AFM with small oscillation amplitude of a cantilever for atomic-resolution imaging of a musco-vite mica substrate in water.[17]

Bacterial plasmid pUC18 (2686 base pairs), which is a closed-circular DNA, was immobilized onto a freshly cleaved muscovite mica substrate, and FM-AFM imag-ing was performed in 50 mM $NiCl_2$ solution. Because both the cleaved surface of muscovite mica and the sugar−phosphate backbone are negatively charged, nickel ions weakly bind DNA onto the mica substrate by electrostatic interactions.[18] The tip−sample distance was regulated by keeping the frequency shift constant at about +80 Hz, which corresponds to the tip−sample interaction force of about +40 pN (Supporting Informa-tion Figures S1−S4).

RESULTS AND DISCUSSION

FM-AFM of Plasmid DNA Revealing the B-Form Structure with Conformational Varieties. A typical FM-AFM topographic image of the plasmid DNA in 50 mM $NiCl_2$ solution is shown in Figure 1A. The plasmid DNA molecules are interwound, as previously reported.[19] In a high-resolution FM-AFM image of the plasmid DNA in the 50 mM $NiCl_2$ solution (Figure 1B; see also Supporting Information Figure S5), deep grooves between the sugar−phosphate backbones of DNA are clearly resolved. We found that two distinct types of grooves with different widths appeared alternately, as partly indicated by the red and blue arrows in Figure 1B, respectively. By carefully mea-suring the groove widths (distances between the adja-cent DNA backbones) along the local helix axis of DNA, two groove widths were quantitatively differentiated (Figure 1C and Supporting Information Figure S6). These grooves are attributed to the major and minor grooves of B-DNA. The sum of the major and minor groove widths, which correspond to the B-DNA helix pitch, was 3.7 nm with a standard deviation of 0.15 nm (Supporting Infor-mation Figure S7). The helix pitch of B-DNA in water has been reported to be 3.6 nm (axial rise: 10.5 bp/turn on average[20]), and this value was determined to be slightly larger than that of the classic Watson−Crick model (3.4 nm) on the basis of an X-ray fiber diffraction study.[1] In addition, plasmid DNA isolated from cells is regularly underwound (negatively supercoiled).[21] Therefore, we conclude that the helix pitch of 3.7 nm with a standard deviation of 0.15 nm observed in our study reflects the nature of real plasmid DNA under physiological condi-tions. Note that there were some regions where the base
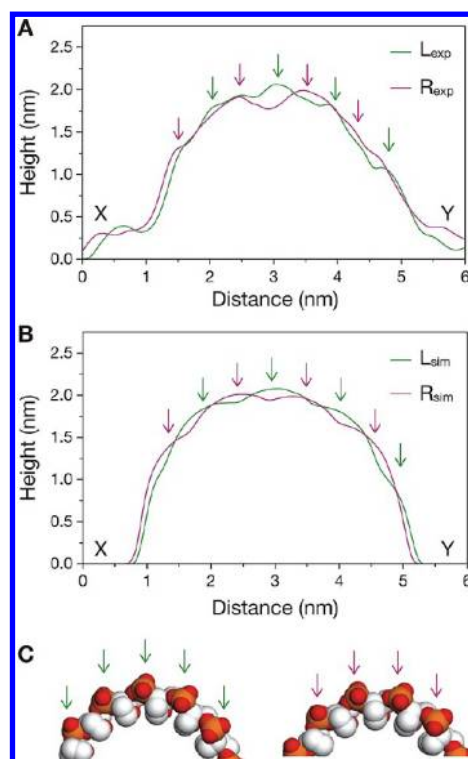

Figure 3. Comparison of cross-sectional profiles along the adjacent DNA backbones in simulated AFM and FM-AFM images (Supporting Information Figures S8 and S9). (A) Cross-sectional profiles along two adjacent sugar−phosphate back-bones in FM-AFM image. L_{exp} and R_{exp} were measured along the left (green) and right (purple) lines in Figure 2A, respec-tively. (B) Cross-sectional profiles along two adjacent sugar−phosphate backbones in a simulated AFM image. L_{sim} and R_{sim} were measured along the left (green) and right (purple) lines in Figure 2D, respectively (see also Supporting Informa-tion Figure S10). (C) Arrangements of the phosphate groups in the DNA backbones. The arrows in both figures indicate locations of protrusions corresponding to the phosphate groups in the DNA backbones.

pairings of DNA were partially melted, as indicated by gray arrows in Figure 1B. The local conformational varia-tions may also be caused by undertwisting of plasmid DNA, and these regions were excluded in the analyses of the groove widths and helix pitch (Supporting Informa-tion Figures S6 and S7).

Comparison with Simulated AFM Images of B-DNA. The area indicated by the rectangle in Figure 1B is magni-fied in Figure 2A. The cross-sectional profile measured along the A−B line in Figure 2A, which is perpendicular to the helix axis, shows the apparent molecular width broadening of B-DNA because of the finite tip radius (Figure 2B). For precise estimation of the tip size, we simulated AFM images of B-DNA with a tip radius of 0.2, 1.0, and 2.0 nm by using the atomic coordinate data of B-DNA obtained from Protein Data Bank (Figure 2C−E; see also the Methods section). The cross-sectional profiles measured along the A−B lines in Figure 2C−E, which are vertical to the helix axes, show different molecular widths (Figure 2F−H). While the full width at half-maximum (fwhm) of the experimental height
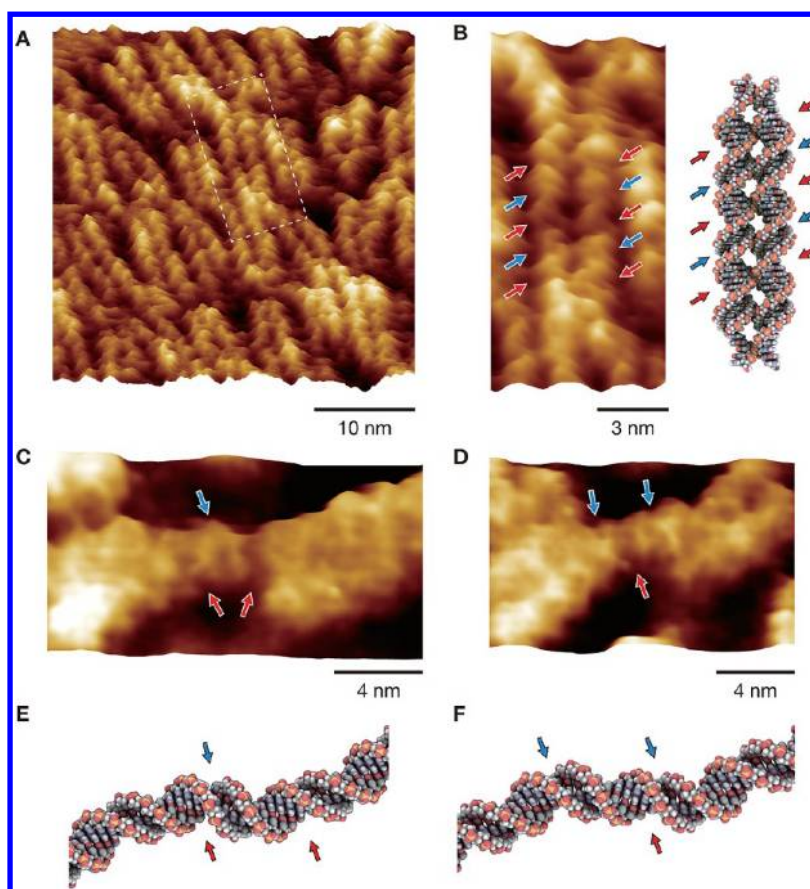
Figure 4. FM-AFM images of the DNA tiles (DAO-E lattice). (A) High-resolution topographic image of the DNA tiles (DAO-E lattice) in aqueous solution (50 mM NiCl$_2$) by FM-AFM. **(B)** Magnified image of the area indicated by the white rectangle in (A) and theoretical model of the DNA tile unit. The red and blue arrows indicate the major and minor grooves of B-DNA, respectively. **(C,D)** Topographic images of the unit connections of the DNA tiles by FM-AFM in aqueous solution (50 mM NiCl$_2$). The red and blue arrows indicate the locations of the major and minor grooves of B-DNA, respectively. **(E,F)** Molecular models of the unit connections of the DNA tiles corresponding to the FM-AFM images in (C,D), respectively.

profile in Figure 2B is about 3.8 nm, the fwhm values of the simulated height profiles in Figure 2F–H are 2.5, 3.6, and 4.4 nm, respectively. By comparing these simulated values with the experimental results, we found that the simulated AFM image with a tip radius of 1.0 nm (Figure 2D,G) was the best simulation. We also found that the angles between the DNA backbones and helix axes in the simulated images increased with increasing tip radius, and the angle in the simulated image (Figure 2D) matches that in the experimental image (Figure 2A). Note that the DNA profile tail in Figure 2B was slightly different from that in Figure 2G. This is assumed to be caused by the adsorbates since the mica surface was partially covered with adsorbates from the NiCl$_2$ solution, such as nickel hydroxides (Ni(OH)$_2$), as shown in Figure 1B. Considering that the nominal tip radius as obtained from the manufacturer was 7 nm and that we routinely resolved the major and minor grooves of B-DNA, it is proposed that an atomically sharp tip with a radius of about 1 nm occasionally formed on the tip apex. This may have contributed to the high-resolution images obtained by FM-AFM.

Positions of Single Functional Groups within DNA Backbones Determined by FM-AFM. The experimental cross-sectional

profiles measured along the two adjacent DNA backbones were compared with corresponding simulated profiles along the neighboring DNA backbones (Figure 3A,B; see also Supporting Information Figures S8 and S9). The phosphate groups are recognized as the protruding corrugations in the simulated profiles (arrows in Figure 3B). The periodic corrugations along the neighboring backbone are slightly out of phase with each other. Correspondingly, we also found the shift of the corrugation phase in the experimental profiles (arrows in Figure 3A). It is strongly suggested that the periodic corrugations in the experimental profile correspond to the individual phosphate groups in the DNA backbones, as modeled in Figure 3C. From additional simulated results using other atomic coordinate data available in the Protein Data Bank, we confirmed that this relative phase shift is the essential feature of B-DNA, independent of the nucleic acid sequence (Supporting Information Figure S10). The measured height of the DNA backbones from the substrate in Figure 3A is about 2 nm. This value agrees well with the diameter of B-DNA (2.0 nm), although it has been reported that the height of B-DNA measured by AFM

was often much less than 2.0 nm because of the sample deformation caused by high tip—sample interaction forces.[22] Therefore, the plasmid DNA was imaged by FM-AFM in aqueous solution without causing deformation.

Submolecular Structure of Self-Assembled DNA Nanostructures Resolved by FM-AFM. Finally, we present results of sub-molecular-scale imaging using FM-AFM of DNA tiles (DAO-E lattice) in an aqueous solution. We obtained an FM-AFM image of the DNA tiles in 50 mM NiCl$_2$ solution (Figure 4A). In a magnified image of the DNA tile unit, the major and minor grooves of B-DNA are successfully resolved (Figure 4B). The angle between the DNA backbones and the helix axis indicates the right-handedness of the B-DNA in the tile. The DNA tile units are connected by Watson—Crick base pairing between sticky ends. The major and minor grooves are also resolved in the FM-AFM images taken on the connecting parts of the DNA tile units (Figure 4C,D). There are two different unit connections in the DAO-E lattice, which are shown as the molecular models in Figure 4E,F. Comparing the FM-AFM images with the models, we suppose that the connections of the DNA chains resolved in Figure 4C,D correspond to two different connecting conformations. The FM-AFM images and models are consistent with a previous report showing that the DNA chains are not straight at the connection but instead have kinks.[23] We concluded that the two different types of unit connections were successfully imaged as the two different major/minor groove arrangements in an aqueous solution. High-resolution visualization by FM-AFM of the crossover structure within the DNA tile unit, which is close to the Holliday junction[24] formed during DNA recombination, is underway to determine the structural differences between the crossover structure and the ideal B-form conformation.

CONCLUSIONS

We used FM-AFM to directly visualize the double helix structure of plasmid DNA in an aqueous solution. The major and minor grooves between the sugar—phosphate backbones of B-DNA were differentiated, and periodic corrugations corresponding to individual phosphate groups in the DNA backbones were resolved. We determined the AFM tip radius as 1.0 nm by comparing the simulated AFM images assuming various tip radii with the FM-AFM image, and the interpretation of the experimental results was validated by the precise comparison of the cross-sectional profiles on the DNA backbones. In addition, we used FM-AFM to perform high-resolution imaging of DNA tiles in an aqueous solution, which showed the right-handedness of B-DNA in the tile and the two different connecting configurations. The results demonstrate the applicability of AFM to sub-molecular-scale investigations of correlations between the structures and functions of DNA under physiological conditions. For example, the approach may allow determination of the structures of various protein—nucleic acid complexes or reveal the mechanisms of sequence recognition by DNA-binding proteins. Finally, it should be noted that the technique presented here is one of the most promising analytical tools for investigating the structures of self-assembled DNA nanostructures, such as DNA tiles and DNA origami, which are being developed for applications in DNA computing and other DNA-based nanoscale devices that use the structures and functions of DNA in solution.

METHODS

Plasmid DNA. Plasmid pUC18 (2686 base pairs, GenBank accession number: L09136) molecules in TE buffer solution (10 mM Tris-HCl, 1 mM EDTA, pH 8.0) were purchased from Takara Bio. We obtained a solution with a concentration of 1.0 ng/μL by dilution with ultrapure water (Millipore). A 20 μL droplet of the DNA solution was deposited onto a freshly cleaved muscovite mica substrate. Fifteen minutes later, the substrate was gently rinsed five times with a solution of 50 mM nickel(II) chloride hexahydrate (NiCl$_2 \cdot$6H$_2$O, 99.9998% purity, Alfa Aesar). We performed FM-AFM imaging in the same 50 mM NiCl$_2$ solution before drying it. The Chimera package (Resource for Biocomputing, Visualization and Informatics, University of California, San Francisco)[25] was used to generate molecular drawings of the sugar—phosphate backbones of plasmid DNA (Figure 3C).

DNA Tile. Synthesized single-stranded DNA (ssDNA) oligomers (HPLC purified) that construct the DAO-E (double-crossover, antiparallel junction, odd intramolecular spacing, even intermolecular spacing) lattice were purchased from BEX. The ssDNA molecules were all dissolved to give concentrations of 0.1 μM in a TE buffer solution, and a thermal cycler (ASTEC) for two-dimensional crystal formation was used to anneal the solution from 90 to 20 °C for 40 h. We deposited the solution of the DNA crystals onto a muscovite mica substrate in the same manner as used in the FM-AFM imaging of the plasmid DNA molecules described above. The atomic coordinate data of the DNA tile unit were provided by Winfree and co-workers (Figure 4B).[26] NAMOT (Nucleic Acid MOdeling Tool)[27,28] was used for building molecular models of the unit connections with DNA curvature[29] in the DNA crystal, and QuteMol (Visual Computing Laboratory, ISTI-CNR)[30] was used to generate molecular drawings of the models (Figure 4E,F).

FM-AFM Imaging. We used customized AFM instruments, JSPM-4200 (JEOL) with an analogue controller and SPM-9600 (Shimadzu) with a home-built digital controller programmed in LabVIEW (National Instruments). The noise-equivalent displacement density was reduced to approximately 20 fm/√Hz by modification of the optics and electronics (Supporting Information Figure S11).[31] We used a silicon cantilever with a Au coating on the backside (PPP-NCHAuD; Nanosensors). The nominal spring constant of the cantilever was 42 N/m. The resonance frequency and quality factor in the solution were about 150 kHz and 7, respectively. The cantilever was self-oscillated at its resonance frequency, and home-built electronics were used to detect the frequency shift.[32] An automatic gain control system (constant amplitude mode) was used to maintain constant oscillation amplitude. The typical oscillation amplitude was 0.4—0.5 nm. Because of

the nonlinearity of the piezoelectric scanner, distances measured by AFM may contain a calibration error of up to about 5%. WSxM (Nanotech Electronica)[33] was used to process all of the AFM images.

Simulation of Topographic AFM Images. GeomAFM Simulator software (version 1.1) in SPM SimSoftware Suite[34] was used to simulate AFM images of B-DNA by calculating the tip trajectory when the outer surface of the conical tip touched and followed the outermost atoms of DNA. The tip was modeled as a sphere with a radius of 0.2, 1.0, or 2.0 nm and a cone with a half cone angle of 10°. Atomic coordinates of B-DNA were obtained from the Protein Data Bank (PDB ID code: 1LAI[35]).

Conflict of Interest: The authors declare no competing financial interest.

Supporting Information Available: Additional figures. This material is available free of charge *via* the Internet at http://pubs.acs.org.

REFERENCES AND NOTES

1. Watson, J. D.; Crick, F. H. C. Molecular Structure of Nucleic Acids. *Nature* **1953**, *171*, 737–738.
2. Binnig, G.; Quate, C. F.; Gerber, C. Atomic Force Microscope. *Phys. Rev. Lett.* **1986**, *56*, 930–933.
3. Hansma, H. G.; Laney, D. E.; Bezanilla, M.; Sinsheimer, R. L.; Hansma, P. K. Applications for Atomic Force Microscopy of DNA. *Biophys. J.* **1995**, *68*, 1672–1677.
4. Mou, J.; Czajkowsky, D. M.; Zhang, Y.; Shao, Z. High-Resolution Atomic-Force Microscopy of DNA: The Pitch of the Double Helix. *FEBS Lett.* **1995**, *371*, 279–282.
5. Maaloum, M. A Close Encounter with DNA. *Eur. Biophys. J.* **2003**, *32*, 585–587.
6. Albrecht, T. R.; Grütter, P.; Horne, D.; Rugar, D. Frequency Modulation Detection Using High-*Q* Cantilevers for Enhanced Force Microscope Sensitivity. *J. Appl. Phys.* **1991**, *69*, 668–673.
7. Giessibl, F. J. Advances in Atomic Force Microscopy. *Rev. Mod. Phys.* **2003**, *75*, 949–983.
8. Kitazawa, M.; Ito, S.; Yagi, A.; Sakai, N.; Uekusa, Y.; Ohta, R.; Inaba, K.; Hayashi, A.; Hayashi, Y.; Tanemura, M. High-Resolution Imaging of Plasmid DNA in Liquids in Dynamic Mode Atomic Force Microscopy Using a Carbon Nanofiber Tip. *Jpn. J. Appl. Phys.* **2011**, *50*, 08LB14.
9. Leung, C.; Bestembayeva, A.; Thorogate, R.; Stinson, J.; Pyne, A.; Marcovich, C.; Yang, J.; Drechsler, U.; Despont, M.; Jankowski, T. Atomic Force Microscopy with Nanoscale Cantilevers Resolves Different Structural Conformations of the DNA Double Helix. *Nano Lett.* **2012**, *12*, 3846–3850.
10. Drew, H. R.; Wing, R. M.; Takano, T.; Broka, C.; Tanaka, S.; Itakura, K.; Dickerson, R. E. Structure of a B-DNA Dodecamer: Conformation and Dynamics. *Proc. Natl. Acad. Sci. U.S.A.* **1981**, *78*, 2179–2183.
11. Winfree, E.; Liu, F.; Wenzler, L. A.; Seeman, N. C. Design and Self-Assembly of Two-Dimensional DNA Crystals. *Nature* **1998**, *394*, 539–544.
12. Bath, J.; Turberfield, A. J. DNA Nanomachines. *Nat. Nanotechnol.* **2007**, *2*, 275–284.
13. Pinheiro, A. V.; Han, D.; Shih, W. M.; Yan, H. Challenges and Opportunities for Structural DNA Nanotechnology. *Nat. Nanotechnol.* **2011**, *6*, 763–772.
14. Saenger, W. *Principles of Nucleic Acid Structure*; Springer-Verlag: New York, 1984.
15. Luger, K.; Mäder, A. W.; Richmond, R. K.; Sargent, D. F.; Richmond, T. J. Crystal Structure of the Nucleosome Core Particle at 2.8 Å Resolution. *Nature* **1997**, *389*, 251–260.
16. Harrison, S. C. A Structural Taxonomy of DNA-Binding Domains. *Nature* **1991**, *353*, 715–719.
17. Fukuma, T.; Kobayashi, K.; Matsushige, K.; Yamada, H. True Atomic Resolution in Liquid by Frequency-Modulation Atomic Force Microscopy. *Appl. Phys. Lett.* **2005**, *87*, 034101.
18. Hansma, H. G.; Laney, D. E. DNA Binding to Mica Correlates with Cationic Radius: Assay by Atomic Force Microscopy. *Biophys. J.* **1996**, *70*, 1933–1939.
19. Hansma, H. G.; Vesenka, J.; Siegerist, C.; Kelderman, G.; Morrett, H.; Sinsheimer, R. L.; Elings, V.; Bustamante, C.; Hansma, P. K. Reproducible Imaging and Dissection of Plasmid DNA under Liquid with the Atomic Force Microscope. *Science* **1992**, *256*, 1180–1184.
20. Rhodes, D.; Klug, A. Helical Periodicity of DNA Determined by Enzyme Digestion. *Nature* **1980**, *286*, 573–578.
21. Boles, T. C.; White, J. H.; Cozzarelli, N. R. Structure of Plectonemically Supercoiled DNA. *J. Mol. Biol.* **1990**, *213*, 931–951.
22. Moreno-Herrero, F.; Colchero, J.; Baro, A. M. DNA Height in Scanning Force Microscopy. *Ultramicroscopy* **2003**, *96*, 167–174.
23. Rothemund, P. W. K.; Papadakis, N.; Winfree, E. Algorithmic Self-Assembly of DNA Sierpinski Triangles. *PLoS Biol.* **2004**, *2*, 2041–2053.
24. Fu, T. J.; Seeman, N. C. DNA Double-Crossover Molecules. *Biochemistry* **1993**, *32*, 3211–3220.
25. Pettersen, E. F.; Goddard, T. D.; Huang, C. C.; Couch, G. S.; Greenblatt, D. M.; Meng, E. C.; Ferrin, T. E. UCSF Chimera—A Visualization System for Exploratory Research and Analysis. *J. Comput. Chem.* **2004**, *25*, 1605–1612.
26. Schulman, R.; Lee, S.; Papadakis, N.; Winfree, E. One Dimensional Boundaries for DNA Tile Self-Assembly. *Lect. Notes Comput. Sci.* **2004**, *2943*, 108–125.
27. Tung, C. S.; Carter, E. S., II. Nucleic Acid Modeling Tool (NAMOT): An Interactive Graphic Tool for Modeling Nucleic Acid Structures. *Comput. Appl. Biosci.* **1994**, *10*, 427–433.
28. Carter, E. S., II; Tung, C. S. NAMOT2: A Redesigned Nucleic Acid Modeling Tool: Construction of Non-canonical DNA Structures. *Comput. Appl. Biosci.* **1996**, *12*, 25–30.
29. Calladine, C. R.; Drew, H.; Luisi, B. F.; Travers, A. A. *Understanding DNA: The Molecule & How It Works*; Academic Press: New York, 2004.
30. Tarini, M.; Cignoni, P.; Montani, C. Ambient Occlusion and Edge Cueing for Enhancing Real Time Molecular Visualization. *IEEE Trans. Visualization Comput. Graphics* **2006**, *12*, 1237–1244.
31. Fukuma, T.; Kimura, M.; Kobayashi, K.; Matsushige, K.; Yamada, H. Development of Low Noise Cantilever Deflection Sensor for Multienvironment Frequency-Modulation Atomic Force Microscopy. *Rev. Sci. Instrum.* **2005**, *76*, 053704.
32. Kobayashi, K.; Yamada, H.; Itoh, H.; Horiuchi, T.; Matsushige, K. Analog Frequency Modulation Detector for Dynamic Force Microscopy. *Rev. Sci. Instrum.* **2001**, *72*, 4383.
33. Horcas, I.; Fernandez, R.; Gomez-Rodriguez, J. M.; Colchero, J.; Gómez-Herrero, J.; Baro, A. M. WSXM: A Software for Scanning Probe Microscopy and a Tool for Nanotechnology. *Rev. Sci. Instrum.* **2007**, *78*, 013705.
34. SPM Sim Software suite was developed by Tsukada, M. and co-workers, under SENTAN Program of the Japan Science and Technology Agency.
35. Weisenseel, J. P.; Reddy, G. R.; Marnett, L. J.; Stone, M. P. Structure of an Oligodeoxynucleotide Containing a 1,N^2-Propanodeoxyguanosine Adduct Positioned in a Palindrome Derived from the *Salmonella typhimurium* hisD3052 Gene: Hoogsteen Pairing at pH 5.2. *Chem. Res. Toxicol.* **2002**, *15*, 127–139.